Effects of Ce substitution and reduction on the electronic states of $Nd_{2-x}Ce_xCuO_{4-y}$ studied by x-ray photoemission

T. Suzuki* and M. Nagoshi
Steel Research Center, NKK Corporation, Kawasaki 210, Japan

Y. Fukuda
Research Institute of Electronics, Shizuoka University, Hamamatsu 432, Japan

K. Oh-ishi, Y. Syono, and M. Tachiki
Institute for Materials Research, Tohoku University, Sendai 980, Japan
(Received 19 March 1990)

The effects of Ce substitution and reduction on the core levels and valence electronic states of $Nd_{2-x}Ce_xCuO_{4-y}$ have been investigated using x-ray photoelectron spectroscopy (XPS). It is found that the surfaces could be tremendously degraded by scraping, leading to changes in the electronic structures of Cu, O, and the Fermi edge. The changes in the Cu $2p$ spectra imply that the Ce substitution and the reduction donate electrons to Cu sites to show the appearance of monovalent Cu. The fraction of monovalent Cu derived from the Cu $2p$ spectra is less than the amount of Ce, which suggests that Ce is in the mixed-valence state. The XPS valence spectra show the Fermi edge formed by the electrons injected into the electronic state with the Cu $3d^{10}$ configuration. The nature of the Fermi edge is discussed in terms of photoionization cross section.

I. INTRODUCTION

Recently Tokura *et al.*[1,2] discovered a new family of cuprate superconductor $Nd_{2-x}Ce_xCuO_{4-y}$ with a Tc of 24 K. The most remarkable characteristic in $Nd_{2-x}Ce_xCuO_{4-y}$ is that, as shown in the Hall coefficient data, the charge carriers are doped electrons (n-type superconductors), in contrast with hole carriers in the conventional cuprate superconductors (p-type superconductors).[1-3] Therefore, it is of great interest to see the differences of the electronic structures between n- and p-type superconductors.

To elucidate carrier doping effects on the electronic structures of $Nd_{2-x}Ce_xCuO_{4-y}$, several spectroscopic measurements such as electron energy-loss spectroscopy (EELS), x-ray absorption (XAS), and photoemission have been carried out. However, the results and the interpretations are not consistent with each other. Nücker *et al.* reported from their EELS data that there is no clear evidence for monovalent Cu caused by the Ce substitution and holes exist at the O sites[4] like the cases of conventional p-type superconductors.[5] However, their result was criticized by showing XAS data which imply that the hole state exists about 1 eV above the Fermi level.[6] Tranquada *et al.*[7] reported from XAS data that the doped electrons fill Cu $3d$ holes, but Alp *et al.*[8] concluded that the electron is injected into a band rather than being localized on each Cu site leading to monovalent Cu. On the other hand, Kosugi *et al.*[9] reported that the Ce substitution yields impurity (localized) states whose interaction and superposition are caused to produce bands like Fermi-liquid states. From XPS, Uji *et al.*,[10] Grassmann *et al.*,[11] and Liang *et al.*[12] reported that the Cu$2p$ core-level spectra show the evidence of monovalent Cu due to the Ce substitution, but Rajumon *et al.*[13] pointed out it is due to covalency effects. On the other hand, Ishii *et al.*[14] pointed out the partial occupation of the Cu$3d$ orbitals from the analysis of the satellite spectral intensity of Cu$2p_{3/2}$. On the contrary, Fujimori *et al.*[15] reported no evidence for the occupation of Cu$3d$ by the doped electrons in XPS and no density of states near the Fermi level in ultraviolet photoelectron spectroscopy (UPS).

We have, for the first time, reported that our XPS data show the clear Fermi edge definitely caused by the electron doping and pointed out that the density of states at the Fermi level consists of Cu $3d$ electrons,[16] which was recently confirmed by resonant and angle-resolved photoemission measurements using synchrotron radiation source.[17,18] The Fermi edge was only observed on the clean-cleaved surface, which suggests the importance of the surface preparation. In photoemission measurements for the high-T_c oxides, mechanical cleaning such as scraping by a file has widely been used. Here we should pay much attention to the surface stability of the samples. In case of Bi-Sr-Ca-Cu-O, the spectra from the scraped surface are considered to be reliable, because the surface of the oxide is substantially stable even if not at a low temperature.[19] However, the scraped surfaces of Y-Ba-Cu-O and La-Sr-Cu-O could be easily deteriorated under ultrahigh vacuum.[19-21] In case of $Nd_{2-x}Ce_xCuO_{4-y}$, the photoemission data reported,[10-15] except for Refs. 16–18, were taken from scraped surfaces, although its surface stability has not been clear. Therefore, we have to be careful about the method to obtain a clean surface being appropriate for the photoemission measurements. We found it is a reliable method for XPS to

 ©1990 The American Physical Society

cleave the sample *in situ* under ultrahigh vacuum conditions even though the sample is polycrystalline.

In this paper, we report the details of our XPS results and discuss the Ce substitution and reduction effects on the electronic structures of $Nd_{2-x}Ce_xCuO_{4-y}$. The contents we discuss here are as follows: (i) Importance of the procedure to obtain a clean surface which is adequate for the XPS measurements; (ii) Ce substitution and reduction effects on the core levels of O1*s*, Nd 3*d*, Ce 3*d*, and Cu 2*p*; (iii) Analysis of the Cu 2*p* core-level spectra and the relationship between the amount of Ce and the fraction of monovalent Cu derived from the Cu 2*p* spectra; (iv) The valence electronic states in the x-ray photoemission spectra.

II. EXPERIMENT

The samples of $Nd_{2-x}Ce_xCuO_{4-y}$ ($x=0$, 0.05, 0.10, 0.15, 0.20, and 0.25) were synthesized by reaction of appropriate amounts of Nd_2O_3, CeO, and CuO, according to a previous paper.[22] The mixed powder was prefired at 950 °C for 12 h in air and they were ground, pressed into pellets,and sintered at 1100 °C for 12 h in air. The superconductive samples with a T_c of 23 K (Fig. 1) were obtained by heating the pellets of $Nd_{1.85}Ce_{0.15}CuO_4$ at 900 °C for 12 h in vacuum ($\sim 10^{-3}$ Pa) and cooled in the vacuum furnace. In this study the vacuum annealing was adopted as the reduction treatment in place of a heat treatment in a low oxygen atmosphere e.g., Ar/O_2 mixture,[1] because we have experienced that an annealing for many hours in the Ar/O_2 mixture could make the sample decomposed.

The oxygen loss y caused by the vacuum annealing was estimated to be 0.038 from the weight loss, which is in good agreement with the value measured by an iodometric titration[2] and thermogravimetry.[22,23] The x-ray powder diffraction patterns showed that the samples in a region of $0 \leq x \leq 0.2$ consisted of a single phase, but a small amount of CeO_2 exists in the sample with $x=0.25$. The lattice parameter of a-axis slightly increased and c axis decreased with Ce doping ($0 \leq x \leq 0.2$) and both were saturated in the region of $x > 0.2$, showing the solubility limit of Ce in this system at about 0.2.

The x-ray photoemission measurements were carried out at room temperature under an ultrahigh vacuum condition ($\sim 10^{-8}$ Pa) by using a SSX-100 spectrometer (Surface Science Instruments) equipped with a sample preparation chamber, in which the samples are scraped by a file or cleaved. Spectra were taken by using a monochromatized x-ray source of Al$k\alpha$ (1486.6 eV) with a spot size of 300 μm in diameter. The total energy resolution (ΔE) of the spectra was 0.36 eV. The stability of the binding energy scale is within ± 0.05 eV.

III. RESULTS AND DISCUSSION

A. Comparison between the cleaved and scraped surface

The morphology of a cleaved surface of $Nd_{1.85}Ce_{0.15}CuO_{4-y}$ (reduced) is shown in Fig. 2. About 90% of the cleaved surface consists of transgranular cleavages and the other consists of voids and grain boundaries. Because of the dominant transgranular cleavages, it could be concluded that the cleaved surface is suitable for the photoemission measurements. As mentioned in Sec. II, the sample reduced in Ar/O_2 mixture does not show this kind of transgranular cleaveages but most of the cleaved surface consists of grain boundaries. It should be emphasized that the inconsistencies of spectroscopic data mentioned in Sec. I might be ascribed to the sample preparation methods.

At first stage of our XPS measurements, we compared the XPS spectra for the scraped and cleaved surface of $Nd_{1.85}Ce_{0.15}CuO_{4-y}$ (reduced). The results for the O1*s* and Cu2*p* core levels and valence spectra are shown in Fig. 3, where any C 1*s* lines were not observed. To clarify the effects induced by scraping on the spectra, the spectra for the cleaved surface were first taken and those for the

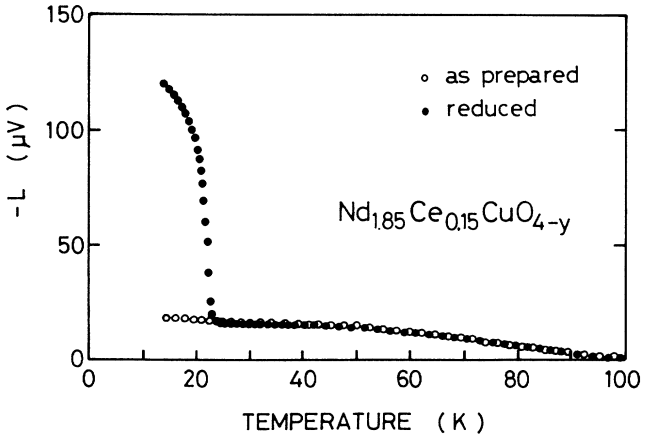

FIG. 1. Inductance as a function of temperature for $Nd_{1.85}Ce_{0.15}CuO_{4-y}$. Open and solid circles show the result of an as prepared (nonsuperconductive) and a reduced (superconductive) sample, respectively. The Meissner signal is observed at 23 K for the reduced sample.

FIG. 2. Scanning electron micrograph of a cleaved surface for $Nd_{1.85}Ce_{0.15}CuO_{4-y}$ (reduced). About 90% of the cleaved surface consists of transgranular cleavages and the other is voids and grain boundaries.

scraped were measured on the same surface. For the cleaved surface, the O1*s* spectrum consists of two peaks as shown in Fig. 3(a), i.e., a sharp strong peak at 528.6 eV and a broad one around 531 eV. The peak around 531 eV are ascribed to contaminations[24–26] which probably exist in the voids or at the grain boundaries. Considering from the morphology of the cleaved surface shown in Fig. 2, the principal peak at 528.6 eV should be ascribed to oxygen in the oxide. We find that the scraping induces a chemical shift for the O1*s* peak at 528.6 eV toward a higher-binding-energy side. We consider that this change in the O1*s* could be ascribed to the considerable structural changes, e.g., many defects or much strain in the crystal structure, because we observed the line broadening in x-ray diffraction for the scraped surface as shown in Fig. 4.

Figure 3(b) shows the Cu2$p_{3/2}$ core-level spectra. The spectrum for the cleaved surface is similar to that of CuO; it consists of the main line at 933.3 eV due to the final state $2p^5 3d^{10}\underline{L}$ ($\underline{L}$ denotes a ligand hole) and the satellite peaks between 940–945 eV due to the final state $2p^5 3d^9$. The spectrum for the scraped surface is considerably changed. The main line is sharpened and shifts toward a lower-binding-energy side, and the satellite peak is weakened. The binding energy of the line is 932.3 eV which is close to the value for Cu_2O (932.0 eV). Hence, this result implies that Cu in the oxide could be reduced by scraping. This might be ascribed to oxygen defects induced by the structural change. We consider that this oxygen loss at the surface is similar to that for La-Sr-Cu-O or Y-Ba-Cu-O.[19–21] Therefore, the scraping could accelerate the oxygen loss in Nd_{2-x} $Ce_x CuO_{4-y}$.

Figure 3(c) shows the valence spectra. It is found that the Fermi edge is dulled by scraping the cleaved surface. This means that the surface is changed from metallic to nonmetallic. Actually, electrical resistance for the scraped surface was about three orders of magnitude larger than that for an unscraped surface.

We here discuss two experimental results: (i) For the scraped surface, the clear Fermi edge was not observed in both XPS (Al $k\alpha$:1486.6 eV) and UPS (He II:40.8 eV),[15] (ii) For the cleaved surface, the Fermi edge was observed in XPS but not in UPS (He I:21.2 eV and HeII, not shown

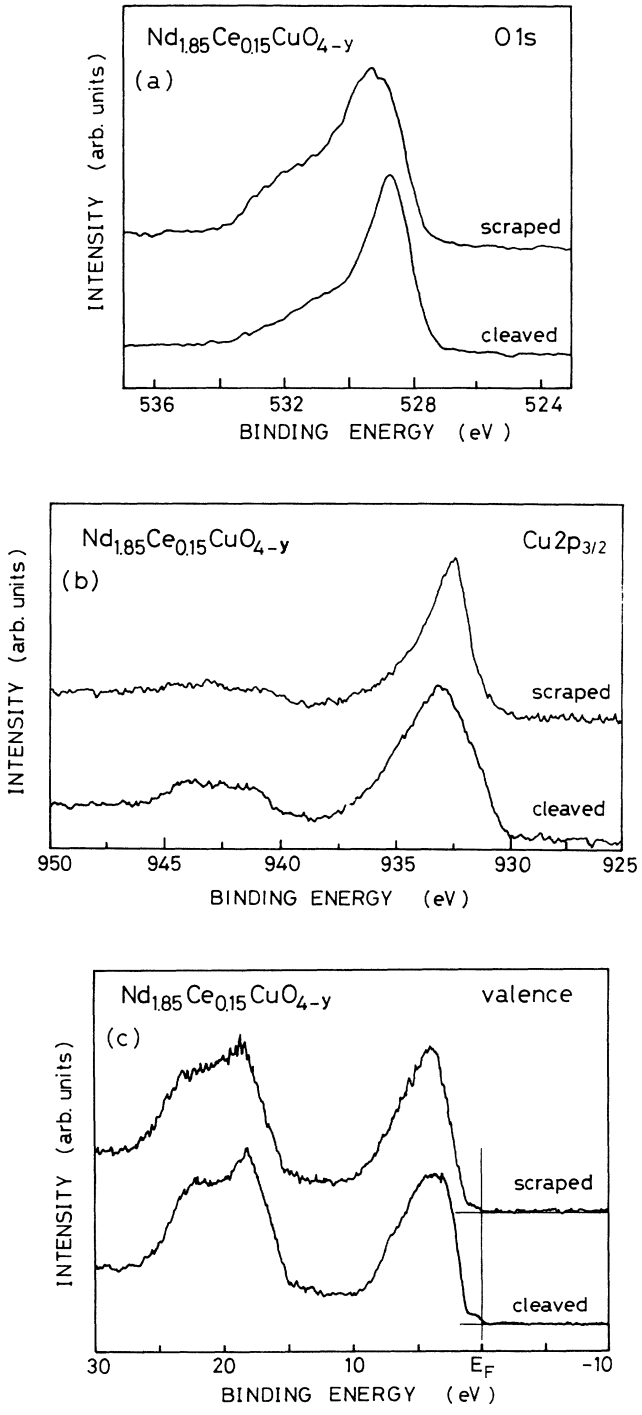

FIG. 3. Effects of scraping by a file on the x-ray photoemission spectra of O1*s* (a), Cu2$p_{3/2}$ (b), and valence states (c) for $Nd_{1.85}Ce_{0.15}CuO_{4-y}$ (reduced). The spectra were taken by scraping the surface cleaved in vacuum.

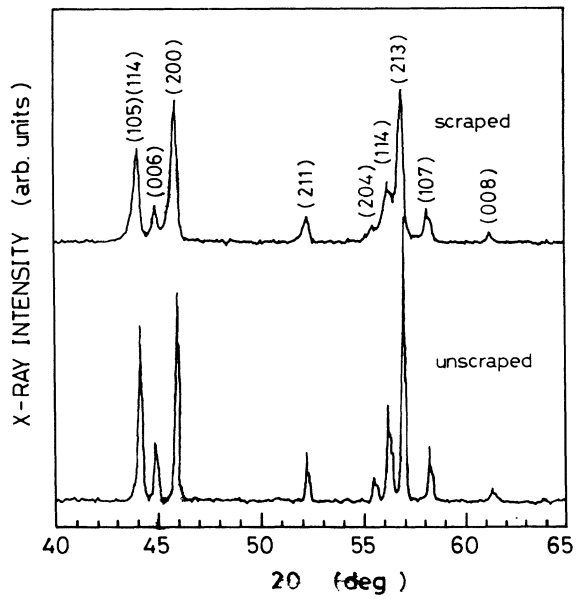

FIG. 4. X-ray diffraction patterns (Cuk_α radiation) for the unscraped and scraped pellets of $Nd_{1.85}Ce_{0.15}CuO_{4-y}$ (reduced).

here). The result (i) is explained by the surface degradation caused by scraping. The result (ii) contradicts an expectation that if the electronic states at the Fermi level originate from Cu 3*d*, the Fermi edge should be more easily observed by using a photon source with a lower energy because of its larger photoionization cross section. However, UPS is more sensitive to the surface than XPS. The escape depth of photoelectrons with the kinetic energy of 1486.6 eV is about one order of magnitude larger than that in the ultraviolet energy range.[27] Therefore, the result (ii) could be explained by assuming a degradation in vacuum, which leads to the requirement of keeping the sample at a low temperature for the UPS measurements.[17,19–21]

B. Ce substitution and reduction effects on the core levels

It is of primary importance to find which elements are affected by the Ce substitution and reduction. Figure 5 shows XPS spectra of the O1*s*, Nd $3d_{5/2}$, and Ce 3*d* core levels for $Nd_{2-x}Ce_xCuO_{4-y}$. The binding energy of O1*s* slightly shifts toward a higher-binding-energy side accompanying the Ce substitution; the O1*s* peak energies for Nd_2CuO_4 and $Nd_{1.8}Ce_{0.2}$ CuO_4 are 528.5 and 528.7 eV, respectively. However, the peak energy of 528.6 eV at $x=0.15$ is not changed by the reduction. This behavior of the O1*s* peak is also observed in the result previously reported.[14] We suppose that the reason for the chemical shift lies in the hybridization effect of the Cu—O and/or Ce—O bonding. This is because the hybridization could make the oxygen valence increased like $O^{2-} \rightarrow O^{(2-q)-}$, which qualitatively agrees with a general tendency of the chemical shift toward a higher-binding-energy side.

As shown in Fig. 5(b), the Nd $3d_{5/2}$ state is affected by neither the Ce substitution nor the reduction. The Nd $3d_{5/2}$ spectrum consist of two peaks ascribed to $4f^3$ and $4f^4\underline{L}$ final states[28] and are exactly the same as that of Nd_2O_3 (trivalent Nd). A peak at 972 eV is due to the $K_1L_{23}L_{23}$ Auger peak of oxygen. Therefore, the valence of Nd in $Nd_{2-x}Ce_xCuO_{4-y}$ is considered to be trivalent.

Figure 5(c) shows the Ce 3*d* core-level spectra which exhibit a characteristic triple-peak structure being similar to that of CeO_2. Two sets of the three peaks denoted by (v_1,v_2,v_3) and (u_1,u_2,u_3) can be ascribed to $3d_{5/2}$ and $3d_{3/2}$, respectively. The Ce 3*d* spectra showed no dependence of the amount of Ce and the reduction treatment. It should be pointed out that the peaks of v_1 and u_1 in the figure are a little broader than those of CeO_2, which suggests that the valence of Ce in $Nd_{2-x}Ce_xCuO_{4-y}$ would be a little different from that in CeO_2. The same feature was observed in the spectra reported in Refs. 10, 13, 15, 29, and 30.

The nominal valence of Ce in CeO_2 is tetravalent. However, it was reported that the triple-peak structure of Ce3*d* in CeO_2 could be explained by considering a mixed-valence state with $4f^0$ and $4f^1$ configurations in the ground state.[31,32] Fujimori[31] concluded that the occupancy of 4*f* state n_f is about 0.6, and the three peaks in the Ce 3*d* spectrum originate from $4f^0$, $4f^1$, and $4f^2$ final states in the photoemission process. On the other hand, Hor *et al.*[30] reported the possibility of the mixed valence of Ce in $Nd_{2-x}Ce_x$ CuO_{4-y} from the analysis of the cell volume, being consistent with their XPS analysis. On the contrary, there are reports showing tetravalent Ce in CeO_2. Wuilloud *et al.*[33] reported that the mixed valence can be excluded in CeO_2, because the empty localized Ce4*f* state within the band gap was observed in the bremsstrahlung isochromat spectroscopy (BIS) data and no density of states was observed at the Fermi level in the XPS data. In $Ln_{2-x}Ce_x$ CuO_{4-y} (Ln:Nd or Gd), Huang *et al.*[34] reported that the valence of Ce is not trivalent but tetravalent from the analysis of the lattice parameters. At present, we cannot estimate the exact valence of Ce in $Nd_{2-x}Ce_xCuO_{4-y}$, but can suggest a possibility of its mixed valence from the analysis of the carrier concentration in the Cu-O planes which will be discussed later.

Figure 6 shows the Cu $2p_{3/2}$ spectra for Nd_{2-x} Ce_xCuO_{4-y}. The systematic variation of the Cu $2p_{3/2}$ spectrum with the Ce substitution is found, that is, the main peak width becomes wider and a peak intensity on the higher-binding-energy side in the satellite peaks decreases. The reduction makes the same effects on the Cu $2p_{3/2}$ spectrum though the magnitude is small. In order to analyze the Cu $2p_{3/2}$ spectral change, a spectrum of Nd_2CuO_4 was subtracted from that of $Nd_{1.85}$ $Ce_{0.15}CuO_{4-y}$ (reduced). The reference spectra for CuO and Cu_2O are displayed in Fig. 7. The subtracted spectrum shows an intense peak at 931.6 eV and a dip at 941.0 eV. The former is similar to the spectrum of Cu_2O (monovalent Cu) in the binding energy and the peak width, which is an evidence of monovalent Cu cuased by the doping.

Furthermore, we calculated spectral intensity ratios of the satellite (I_{sat}) to the main Cu $2p_{3/2}$ peaks (I_{main}) for CuO and $Nd_{2-x}Ce_xCuO_{4-y}$. The results are listed in Table I. It should be noted that the I_{sat}/I_{main} for Nd_2CuO_4 is smaller than that for CuO, and the Ce substitution and reduction make the value decreased. These experimental results could lead us to a conclusion that monovalent Cu increases and divalent Cu decreases with the Ce substitution and reduction, which exactly shows the electron doping to the Cu sites.

From the Cu$2p_{3/2}$ spectra, the fractions of monovalent Cu in $Nd_{2-x}Ce_xCuO_{4-y}$ were estimated by spectral intensity ratios of the peak at 931.6 eV for $Nd_{2-x}Ce_xCuO_{4-y}$ to the total peaks (main plus satellite) for Nd_2CuO_4. The result is displayed in FIg. 8. They are almost proportional to x in $Nd_{2-x}Ce_xCuO_{4-y}$ up to $x=0.2$ and saturate in the region of x more than 0.2. This tendency agrees with the fact that the solubility limit of Ce is about 0.2. It is interesting to examine whether x in $Nd_{2-x}Ce_xCuO_4$ (as prepared) is equal to the fraction of monovalent Cu or not, because if Ce is tetravalent, it is expected that a Cu accepts the electron xe^- in average. Our data indicate that the fractions of monovalent Cu for as prepared samples (open circles in Fig. 8) are less by about 20% than x in $Nd_{2-x}Ce_xCuO_4$ ($0.05 \leq x \leq 0.2$). We suggest that the reason lies in Ce whose valence is less than 4+ due to its mixed valence. The fraction of mono-

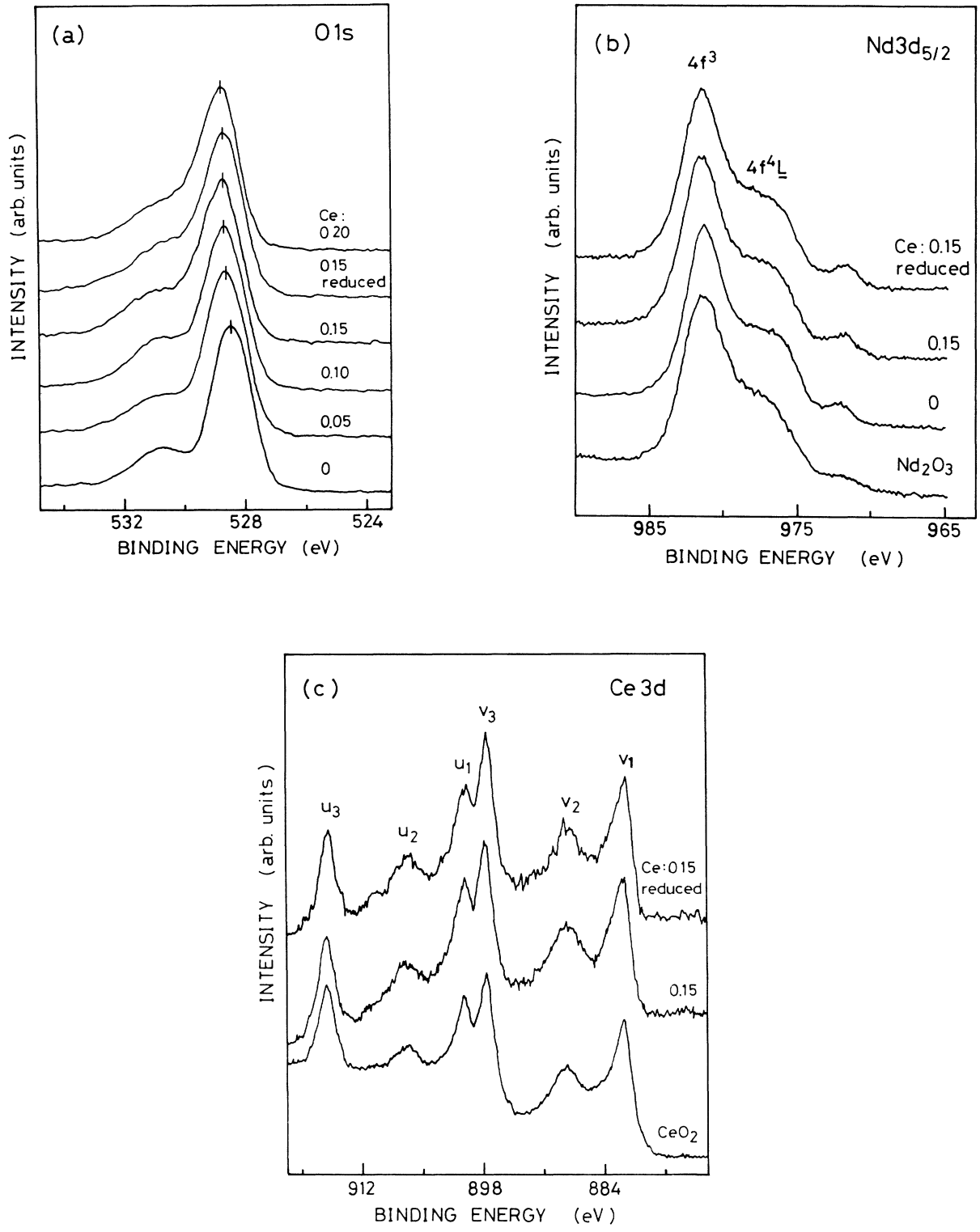

FIG. 5. X-ray photoemission spectra of O1*s* (a), Nd3$d_{5/2}$ (b), and Ce3*d* (c) taken from the cleaved surface of $Nd_{2-x}Ce_xCuO_{4-y}$. The Nd3$d_{5/2}$ and Ce3*d* reference spectra of Nd_2O_3 (trivalent Nd) and CeO_2 (formally tetravalent Ce) are also displayed in figures (b) and (c), respectively. In the O1*s* spectra, the shoulders on the higher-binding-energy side are ascribed to contaminations. Each Nd3$d_{5/2}$ spectrum consists of two peaks due to the $4f^3$ and $4f^4\underline{L}$ final states. A peak at 972 eV due to the $K_1L_{23}L_{23}$ Auger peak of oxygen. Each Ce3*d* spectrum exhibits the three-peak structure, where v_1, v_2, and v_3 belong to Ce3$d_{5/2}$ and u_1, u_2, and u_3 to Ce3$d_{3/2}$. The spectra are normalized by the peak height of v_1.

TABLE I. Spectral intensity ratios of the satellite to the main peaks of Cu $2p_{3/2}$ (I_{sat}/I_{main}) for CuO and $Nd_{2-x}Ce_xCuO_{4-y}$. The deviation for each value is about ±0.015.

CuO	$Nd_{2-x}Ce_xCuO_{4-y}$						
	$x=0$	0.05	0.10	0.15	0.15[a]	0.20	0.25
0.49	0.41	0.40	0.38	0.33	0.31	0.28	0.29

[a] Reduced.

valent Cu for $Nd_{1.85}Ce_{0.15}CuO_{4-y}$ (reduced) is larger by about 0.045 than that for $Nd_{1.85}$ $Ce_{0.15}CuO_4$ (as prepared). This value is in good agreement with the oxygen deficiency mentioned in Sec. II, which is necessary for realizing the superconductivity in this system.

C. Valence states

The valence spectra taken by x-ray photoemission are displayed in Fig. 9. A broad peak between 1 and 8 eV is mainly ascribed to the Cu $3d$ valence states by taking account of the photoionization cross section at 1486.6 eV.[35] The valence band is also mixed with O$2p$ orbitals because the strong valence band was observed by He I photoemission. The weak structures between 9 and 14 eV are considered to be the satellite structures due to the $3d^8$ final state. The intensity of the $3d^8$ satellite peaks is weakened by the Ce substitution, which is consistent with the suppression of the divalent Cu found in Fig. 8. The most important result we should pay attention to is that a density of states at the Fermi level increases and the clear Fermi edge is formed by increasing the Ce substitution. The appearance of this electronic state shows that the system becomes metallic, which agrees with the results of electronic transport measurements.[1,2,36] The Fermi edge is not observed through a resonant photoemission but a normal photoemission process, because there are no electronic states near 1486.6 eV for the system. It is important to know whether the electrons are injected into Cu $3d$ or $4s$ orbitals. We have already mentioned that the Ce substitution and the reduction decrease the $3d^9$ satellite peak intensity in the Cu $2p_{3/2}$ spectrum. From this result the additional electrons are considered to be injected mainly into the Cu sites leading to $3d^{10}$ character in the Cu $3d$–O $2p$ hybridization. We can guess that there could be not only the Cu $3d$ state but also the Cu $4s$ or Ce $4f$ states at the Fermi level. If the mixed valence of Ce is assumed, the Ce $4f$ level may be close to the Fermi level. However, it is suggested that the Cu $4s$ or Ce $4f$ state could not be clearly observed in XPS, because the photoionization cross section[35] at 1486.6 eV for both Cu $4s$

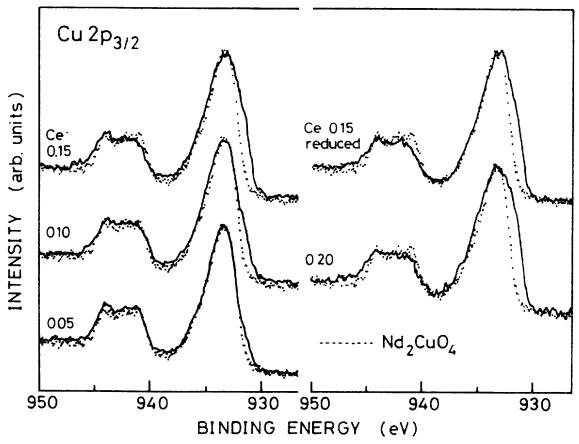

FIG. 6. X-ray photoemission spectra of Cu$2p_{3/2}$ for the cleaved surface of $Nd_{2-x}Ce_xCuO_{4-y}$. Each spectrum exhibits a satellite peak due to the $3d^9$ final state. The dotted curve shows the spectrum for Nd_2CuO_4. The spectra are normalized to the main peak height. The satellite and main peaks are systematically changed by the Ce substitution and reduction.

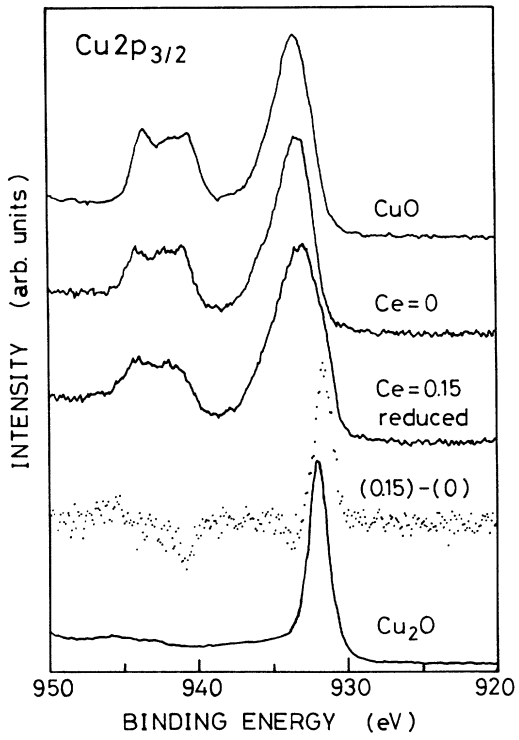

FIG. 7. Cu$2p_{3/2}$ spectra for CuO, Nd_2CuO_4, $Nd_{1.85}Ce_{0.15}CuO_{4-y}$ (reduced), and Cu_2O. To clarify the effects of the Ce substitution and reduction on the spectrum, a subtracted spectrum (dotted curve) for Nd_2CuO_4 (as prepared) from that for $Nd_{1.85}Ce_{0.15}CuO_{4-y}$ (reduced) is displayed. The increase of photoemission intensity at 931.6 eV in the main peak and the decrease around 941 eV in the satellite peak are observed.

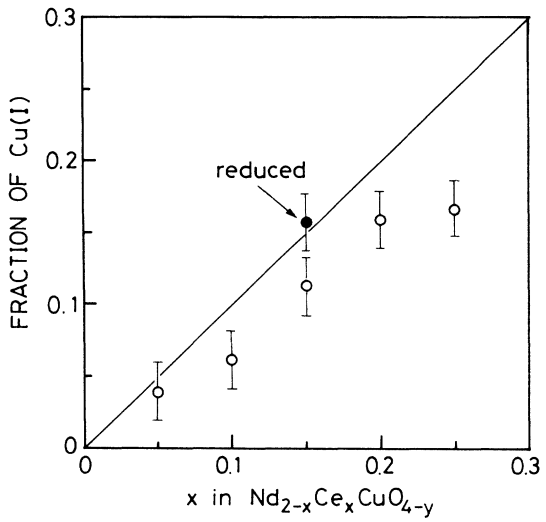

FIG. 8. Relationship between x in $Nd_{2-x}Ce_x$ CuO_{4-y} and the fraction of monovalent copper. Open and solid circles, respectively, show the as prepared and the reduced samples.

(0.00027 Mb) and Ce $4f$ (0.0022 Mb) is about one or two orders of magnitude less than that for Cu $3d$ (0.012 Mb). To find the exact assignment for the electronic states at the Fermi level, it is necessary to carry out resonant photoemission measurements by using synchrotron radiation.

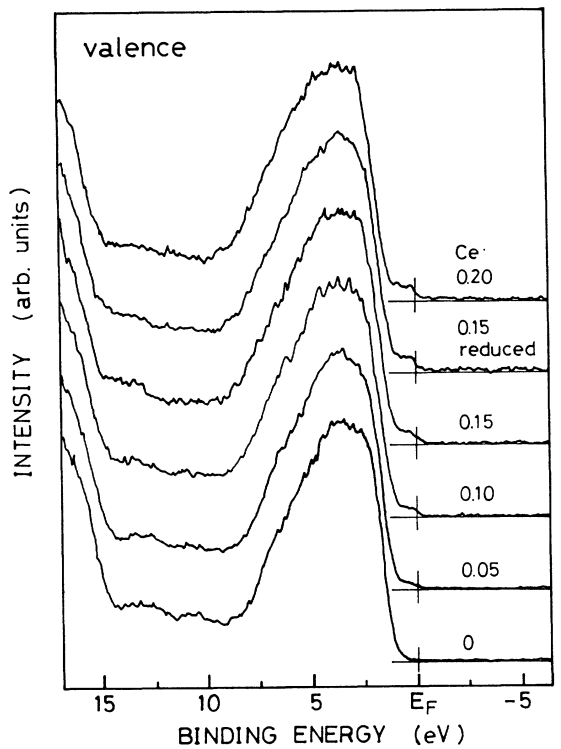

FIG. 9. X-ray photoemission spectra of the valence states for $Nd_{2-x}Ce_xCuO_{4-y}$. The density of states at the Fermi level systematically increases with the Ce substitution. The broad peak between 1 and 8 eV is ascribed to mainly Cu$3d$-O$2p$ hybridization. The weak satellite structures due to the $3d^8$ final state are observed between 9 and 14 eV, of which intensity decreases with the Ce substitution.

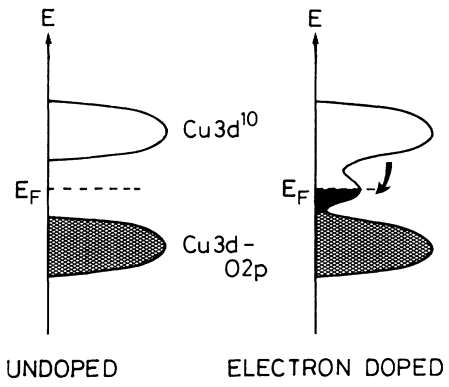

FIG. 10. Schematic illustration of the band scheme in the undoped insulator oxide and the electron-doped superconductive oxide.

Just after we finished writing this manuscript, we have had two preprints concerning a resonant photoemission study[17] and an angle-resolved photoemission study[18] for this system. Allen *et al.*[17] carried out the photoemission measurement at a low temperature using a cleaved single-crystal surface. They found the enhancement of the Fermi edge at a photon energy of 72 and 122 eV showing Cu $3p \rightarrow 3d$ and Ce $4d \rightarrow 4f$ resonances, respectively. The spectral intensity at the Fermi level due to the Cu $3p \rightarrow 3d$ resonance is much stronger than that due to the Ce $4d \rightarrow 4f$ resonance. On the other hand, Sakisaka *et al.*[18] carried out their experiment at 300 K using a clean surface of single-crystal thin film. They found the clear Fermi edge and a dispersive Fermi-liquid state with a strong Cu $3d$ character. These results are completely consistent with our interpretations.

Figure 10 shows a schematic electronic band structure for electron-doped $Nd_{2-x}Ce_xCuO_{4-y}$. A charge-transfer gap opens in undoped Nd_2CuO_4 because of a large Coulomb energy of Cu $3d$ electrons. Electrons doped into this system are accommodated in unoccupied Cu $3d$ orbitals, which would lead to creating a narrow band in the gap and to forming the Fermi edge. The similar theoretical results were reported in hole-doped systems;[37] a narrow band appeared in the band gap by addition of holes into insulators, although in this case the band consists of mainly O $2p$ orbitals. We would like to emphasize here that these narrow bands created by addition of holes or electrons into insulators participate in the high-T_c superconductivity.

IV. SUMMARY

We carried out the x-ray photoemission measurements for Nd_{2-x} Ce_xCuO_{4-y} to elucidate the effects of Ce substitution and reduction on the electronic structures. We suggested that inconsistencies among the published spectroscopic data were due to sample preparations. In the present study, the measurements are carried out for surfaces which show transgranular cleavages. We find that the scraping with a file, which has been widely used, make the sample surface degraded.

The Cu $2p$ core levels in XPS show that the component

of monovalent Cu with the $3d^{10}$ configuration appears with the Ce doping. The fraction of monovalent Cu derived from the Cu $2p$ spectra is about 20% less than x in Nd_{2-x} Ce_xCuO_{4-y} ($0.05 \leq x \leq 0.2$), which suggests that Ce in the system has the mixed valent state.

The valence spectra in XPS show that a density of states at the Fermi level appears with the Ce doping. This behavior is consistent with the changes of the Cu $2p$ core-level spectra, which implies that the electronic states at the Fermi level are ascribed to the electrons injected into the Cu sites with $3d$ character.

ACKNOWLEDGMENTS

This work was supported by the Grant in Aid for Scientific Research on *Chemistry of New Superconductors* (Y.F.) and *Mechanism of Superconductivity* (Y.S. and M.T.) from the Ministry of Education, Science and Culture of Japan.

---

*Present address: Electronic Device Research Dept., Electronic Research Center, NKK Corporation, 9-38 Shoseimachi 2, Shinminato, Toyama 934, Japan.

[1]Y. Tokura, H. Takagi, and S. Uchida, Nature **337**, 345 (1989).

[2]H. Takagi, S. Uchida, and Y. Tokura, Phys. Rev. Lett. **62**, 1197 (1989).

[3]S. Uchida, H. Takagi, Y. Tokura, N. Koshihara, and T. Arima, in *Strong Correlation and Superconductivity,* Proceedings of the IBM Japan International Symposium, Mt. Fuji, Japan, May 21–25, 1989, edited by H. Fukuyama, S. Maekawa, and A. P. Malozemoff (Springer-Verlag, Berlin, 1989), p. 194.

[4]N. Nücker, P. Adelmann, M. Alexander, H. Romberg, S. Nakai, J. Fink, H. Rietschel, G. Roth, H. Schmidt, and H. Spille, Z. Phys. B **75**, 421 (1989); J. Fink, N. Nücker, H. Romberg, M. Alexander, S. Nakai, R. Manzke, T. Buslaps, and R. Claessen, in *Proceedings of the International Winterschool on Electronic Properties of Polymers and Related Compounds, Kirchberg, Austria* (Springer Series in Solid State Science, in press).

[5]N. Nücker, J. Fink, J. C. Fuggle, P. J. Durham, and W. M. Temmerman, Phys. Rev. B **37**, 5158 (1988); N. Nücker, H. Romberg, X. X. Xi, J. Fink, B. Gegenheimer, and Z. X. Zhao, *ibid.* **39**, 6619 (1989).

[6]T. Takahashi, H. Katayama-Yoshida, and H. Matsuyama, Z. Phys. B **78**, 343 (1990).

[7]J. M. Taranquada, S. M. Heald, A. R. Moodenbaugh, G. Liang, and M. Groft, Nature **337**, 720 (1989).

[8]E. E. Alp, S. M. Mini, M. Ramanathan, B. Dabrowski, D. R. Richards, and D. G. Hinks, Phys. Rev. B **40**, 2617 (1989).

[9]N. Kosugi, Y. Tokura, H. Takagi, and S. Uchida, Phys. Rev. B **41**, 131 (1990).

[10]S. Uji, M. Shimoda, and H. Aoki, Jpn. J. Appl. Phys. **28**, L804 (1989).

[11]A. Grassmann, J. Schlötterer, J. Ströbel, M. Klanda, R. L. Johnson, and G. Saemann-Ischenko, in *Proceedings of International Conference Materials and Mechanisms of Superconductivity High-Temperaure Superconductors II, Stanford, U.S.A., July 23–28 1989,* edited by N. E. Phillips, R. N. Shelton, and W. A. Harrison (North-Holland, Amsterdam, 1989).

[12]G. Liang, J. Chen, M. Croft, K. V. Ramanujachary, M. Greenblatt, and M. Hedge, Phys. Rev. B **40**, 2646 (1989).

[13]M. K. Rajumon, D. D. Sarma, R. Vijayaraghavan, and C. N. R. Rao, Solid State Commun. **70**, 875 (1989).

[14]H. Ishii, T. Koshizawa, H. Kataura, T. Hanyu, H. Takai, K. Mizoguchi, K. Kume, I. Shiozaki, and S. Yamaguchi, Jpn. J. Appl. Phys. **28**, L1952 (1989).

[15]A. Fujimori, Y. Tokura, H. Eisaki, H. Takagi, S. Uchida, and E. Takayama-Muromachi, Phys. Rev. B **42**, 620 (1990).

[16]Y. Fukuda, T. Suzuki, M. Nagoshi, Y. Syono, K. Oh-ishi, and M. Tachiki, Solid State Commun. **72**, 1183 (1989).

[17]J. W. Allen, C. G. Olson, M. B. Maple, J. -S. Kang, L. Z. Liu, J. -H. Park, R. O. Anderson, W. P. Ellis, J. T. Markert, Y. Dalichaouch, and R. Liu, Phys. Rev. Lett. **29**, 595 (1990).

[18]Y. Sakisaka, T. Murayama, H. Kato, K. Edamoto, M. Okusawa, Y. Aiura, H. Yamashita, T. Terashima, Y. Bando, K. Kijima, K. Yamamoto, and K. Hirata, Solid State Commun. **74**, 609 (1990).

[19]A. J. Arko, R. S. List, Z. Fisk, S. -W. Cheong, J. D. Thompson, J. A. O'Rourke, C. G. Olson, A. -B. Yang, T. -W. Pi, J. E. Schirber, and N. D. Shinn, J. Magn. Magn. Mater. **75**, L1 (1989).

[20]T. Takahashi, F. Maeda, H. Arai, H. Katayama-Yoshida, Y. Okabe, T. Suzuki, S. Hosoya, A. Fujimori, T. Shidara, T. Koike, T. Miyahara, M. Onoda, S. Shamoto, and M. Sato, Phys. Rev. B **36**, 5686 (1987).

[21]T. Takahashi, F. Maeda, S. Hosoya, and M. Sato, Jpn. J. Appl. Phys. **26**, L349 (1987).

[22]K. Oh-ishi, M. Kikuchi, Y. Syono, N. Kobayashi, and Y. Muto, J. Solid State Chem. **83**, 237 (1989).

[23]K. Oh-ishi, Y. Syono, M. Kikuchi, N. Kobayashi, and Y. Muto, Solid State Commun. **73**, 341 (1990).

[24]A. G. Schrott, S. L. Cohen, T. R. Dinger, F. J. Himpsel, J. A. Yarmoff, K. G. Frase, S. I. Park, and R. Purtell, in *Thin Film Processing and Characterization of High-Temperature Superconductors,* Proceedings of the American Vacuum Society Topical Conference on Thin Film Processing and Characterization of High-T_c Superconductors, AIP Conf. Proc. No. 165, edited by J. M. E. Harper, R. J. Colton, and L. C. Feldman (AIP, New York, 1989), p. 349.

[25]J. H. Thomas III and M. E. Labis, in *Thin Film Processing and Characterization of High-Temperature Superconductors,* Ref. 24, p. 374.

[26]Y. Fukuda, M. Nagoshi, T. Suzuki, Y. Namba, Y. Syono, and M. Tachiki, Phys. Rev. B **39**, 11 494 (1989).

[27]M. P. Seah and W. A. Dench, Surf. Inserf. Anal. **1**, 2 (1979).

[28]J. C. Fuggle, M. Campagna, Z. Zolnierek, R. Lasser, and A. Piatau, Phys. Rev. Lett. **45**, 1597 (1980).

[29]Y. Tokura, A. Fujimori, H. Matsubara, H. Watanabe, H. Takagi, S. Uchida, M. Sakai, H. Ikeda, S. Okuda, and S. Tanaka, Phy. Rev. B **39**, 9704 (1989).

[30]P. H. Hor, Y. Y. Xue, Y. Y. Sun, Y. C. Tao, Z. J. Huang, W. Rabalais, and C. W. Chu, Physica C **159**, 629 (1989).

[31]A. Fujimori, Phys. Rev. B **27**, 3992 (1983); **28**, 2281 (1983); **28**, 4489 (1983).

[32]A. Kotani, H. Mizuta, T. Jo, and J. C. Parlebas, Solid State Commun. **53**, 805 (1985); A. Kotani, in *Core-Level Spectroscopy in Condensed Systems,* Proceedings of the Tenth Taniguchi International Symposium, Kashikojima, Japan, October 19–23, 1987, edited by J. Kanamori and A. Kotani (Springer-Verlag, Berlin, 1988), p. 3; T. Jo and A. Kotani, *ibid.*, p. 34.

[33]E. Wuilloud, B. Delley, W. -D. Schneider, and Y. Bear, Phys.

Rev. Lett. **53**, 202 (1984).
[34]T. C. Huang, E. Moran, A. I. Nazzal, and J. B. Torrance, Physica C **158**, 148 (1989).
[35]J. J. Yeh and I. Lindau, At. Data Nucl. Data Tables **32**, 1 (1985).
[36]S. Uji, H. Aoki, and T. Matsumoto, Jpn. J. Appl. Phys. **28**, L563 (1989).
[37]M. Tachiki, in *Strong Correlation and Superconductivity,* edited by H. Fukuyama, S. Maekawa, and A. P. Malozemoff, Proceedings of the IBM Japan International Symposium, Mt. Fuji, Japan, May 21–25, 1989 (Springer-Verlag, Berlin, 1989), p. 138.

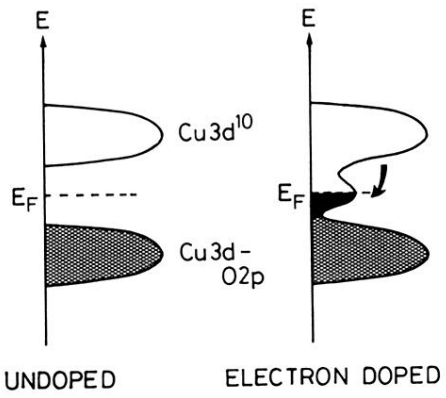

FIG. 10. Schematic illustration of the band scheme in the undoped insulator oxide and the electron-doped superconductive oxide.

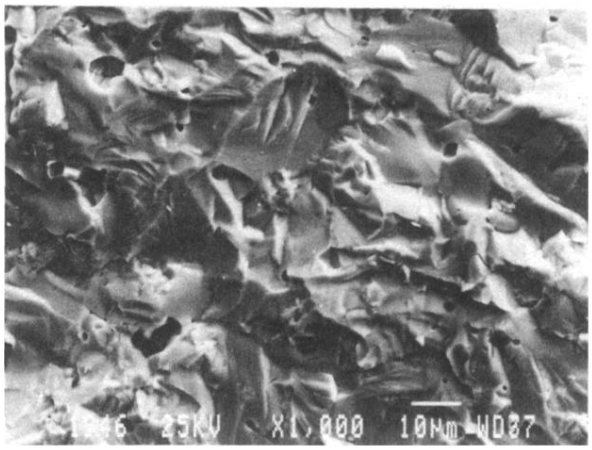

FIG. 2. Scanning electron micrograph of a cleaved surface for $Nd_{1.85}Ce_{0.15}CuO_{4-y}$ (reduced). About 90% of the cleaved surface consists of transgranular cleavages and the other is voids and grain boundaries.